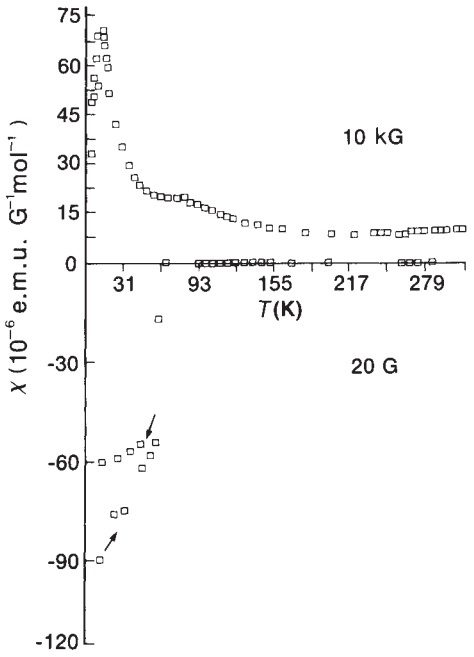

Fig. 3 Temperature dependence of the magnetic susceptibility of the same sample as in Fig. 2*b*, measured at 10 kG and 20 G. The arrows pointing to increasing and decreasing temperature in the lower diagram represent the exclusion and expulsion (Meissner) experiments, respectively.

slowly cooled. The observed localization below ~100 K is also shown by a similarly prepared Y 3-3-6 at $x = 0.375$. After annealing the same samples in 3 atm O_2 at 520 °C, both specimens show a superconductive transition onset near 80 K. Figure 2*b* shows the data for Y 3-3-6, $x = 0.5$, in which a resistive transition onset near 80 K and a shoulder at 60 K can be seen. Figure 3 shows d.c. susceptibility data for the same high-pressure-annealed sample, measured with a SQUID magnetometer at magnetic fields of 10 kG and 20 G. In low field, both exclusion and expulsion experiments indicate the onset of superconductivity below 60 K in a small (1-5%) volume fraction of the sample. This result is similar to that observed in some samples of $La_2CuO_{4-\delta}$[11,12]. The high-field data suggest strong localization below 30 K, with a singularity at 60 K corresponding to the onset of the diamagnetic signal in the low-field data. The same sample, when annealed in 10 atm O_2, shows no indication of a superconducting fraction. These results suggest that when the oxygen content is greater than seven oxygens per formula unit in the Y 3-3-6 structure, the crucial Cu-O chains of the Y 1-2-3 lattice are disrupted, resulting in a loss of bulk superconductivity in the material. Some chain ordering in a minority component of the sample may result in the filamentary superconductivity observed on annealing near an optimal O_2 pressure of 3 atm.

Received 24 November; accepted 29 December 1987.

1. Wu, M. K. *et al. Phys. Rev. Lett.* **58**, 907-911 (1987).
2. David, W. I. F. *et al. Nature* **327**, 310-312 (1987).
3. Siegrist, T., Sunshine, S., Murphy, D. W., Cava, R. J. & Zahurak, S. M. *Phys. Rev.* B**35**, 7137-7140 (1987).
4. David, W. I. F. *et al. Nature* **328**, 328-329 (1987).
5. Torardi, C. C. *et al. Mater. Res. Bull.* (in the press).
6. Maeda, A. *et al. Jap. J. appl. Phys.* **26**, L1366-L1368 (1987).
7. Segre, C. U. *et al. Nature* **329**, 227-229 (1987).
8. Er-Rakho, L., Michel, C., Provost, J. & Raveau, B. *Solid St. Chem.* **37**, 151-156 (1981).
9. Rao, C. N. R., Ganguly, P., Raychandhuri, A. K., Mohan Ram, R. A. & Sreedhar, K. *Nature* **326**, 856-857 (1987).
10. Santoro, A. *et al. Mater. Res. Bull.* **22**, 1007-1013 (1987).
11. Grant, P. M. *et al. Phys. Rev. Lett.* **58**, 2482-2485 (1987).
12. Kang, W. *et al. J. Phys. Paris* **48**, 1181-1186 (1987).

The formation of quasi-icosahedral spiral shell carbon particles

H. W. Kroto & K. McKay

School of Chemistry and Molecular Sciences, University of Sussex, Brighton, Sussex BN1 9QJ, UK

A simple, new, carbon nucleation scheme has been developed which results in quasi-single crystal particles of concentric, spiral-shell internal structure and overall quasi-icosahedral shape. Intermediates consisting of curved graphitic networks and overall growth controlled by epitaxy are key factors in the scheme which also produces buckminsterfullerene, C_{60}^B, as an inert by-product. The scheme which explains, for the first time, the occurrence of polyhedral carbonaceous particles may also apply to soot and circumstellar dust formation.

Until recently it has been assumed that carbonaceous particles such as soot form by high-temperature carbonization of liquid hydrocarbon droplets, the shapes of which are governed by surface tension. This view has been modified by transmission electron microscopy (TEM)[1-3] showing the particles as regular concentric graphitic shells. Similar structures have been found in condensed carbon[4] for which a liquid step seems improbable. This similarity suggests the formation mechanisms are related. Tesner[5] argues that some form of 'chemical crystallization' must be invoked to explain the regular structure of soot. The discovery of the superstable C_{60} molecule with properties consistent with a closed, truncated, icosahedral sphere[6] has led to a new description of a family of hollow-cage carbon species (fullerenes)[7]. A scheme has also been suggested[8] for the formation of C_{60}^B and also of macroscopic carbon particles. Here we discuss a refined nucleation scheme that explains why polyhedra develop. The study further supports the proposal that C_{60}^B is indeed a closed cage[6].

The nucleation scheme rests on the validity of the fullerene proposal and its implications. Traditionally, extended carbon aggregates are expected to involve flat, hexagonal graphitic networks, and it is proposed that the exceptional stability of C_{60}^B is consistent with the closure of such a network and the consequent elimination of the reactive edge of an open sheet. A purely hexagonal network cannot close perfectly, but if 12 pentagons are incorporated it can, although the number of hexagons is arbitrary[9,10,11]. Chemical and geodesic arguments indicate the fullerenes should be stable[7,12,13] and that the set with 24, 28, 32, 50, 60 and 70 atoms would be particularly stable[7], consistent with observation. C_{60}^B is predicted to be uniquely stable because it is the first cage to avoid abutting pentagons, it is highly aromatic, and its high symmetry enables it to distribute strain perfectly in a way available to no other 5/6-ring cage.

Most important is the proposal that carbon nucleation can lead to cages spontaneously. The first key element in the process is the formation of curved 5/6-ring networks by the energy-driven urge to eliminate edge-dangling bonds. In such a chaotic aggregation process the pentagons, which are crucial for curvature, are likely to be dispersed more or less randomly, producing structures such as those in Fig. 1. Occasionally however, they will occur at just the correct place for perfect closure, producing C_{60}^B (ref. 6) or other fullerenes[7]. Without a reactive edge, fullerenes should not grow further but should remain intact in a cul-de-sac while the unclosed shells, presumably the majority, race on to form large particles. The fullerenes are unsuitable sites for further growth and so C_{60}^B will not generally be found at the centre of a carbon particle. Later closure by annealing or accidental entrapment should not, however, be ruled out. For most clusters the advancing edges will miss (Fig.

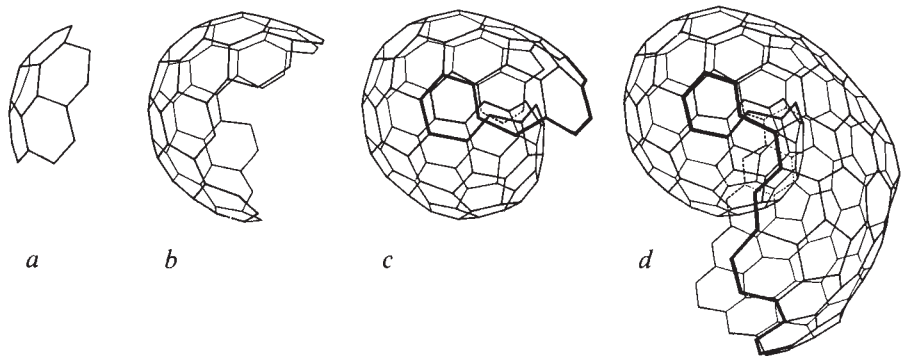

Fig. 1 Hypothetical initial growth sequence evolving from: *a*, a corannulene carbon framework through *b*, and *c*, species in which edge by-pass occurs to *d*, an embryo in which the second shell is forming. The sequence leads in a natural way to both carbon particles and closed cages, fullerenes.

1*c*), and once overlapped, closure is impossible and further rapid growth is predicted to be like a snowball accreting a more or less continuous spiral layer (Fig. 1*d*). Accreting species, on collision with the energy-absorbent surface of the embryo, should be adsorbed and rapidly assimilated into the advancing skin.

The model needs to be refined to deduce structural details. (1) The curvature of the initial embryo should be governed by the 5/6-ring energetics of a free sheet under the condensation conditions that obtain and, although fairly round at first, rather abruptly angled facets may develop, particularly when edge overlap occurs. (2) As accreting species become bonded into the advancing network, pentagons should be located at strategic points so that fresh surface can follow the underlying convex contours, optimized for the graphite interlayer separation (3.4 Å). An important consequence is that new pentagons in the fresh layer should form directly above those in the layer immediately below, so propagating structural integrity. Thus the pentagons should stack epitaxially in columns along twelve radii. (3) As the spirals grow and their sizes become large relative to the interlayer spacing, the overall shapes should approximate to those of closed cages of similar dimensions. Interlayer adhesion, which may be important, is neglected in this preliminary study. (4) Various types of discontinuity should occur. For instance two helical edges propagate as the spiral grows. In Fig. 1 the skew axes are opposed, so the edges spiral away from each other. Normally random discontinuities in the network probably also occur, spoiling the quality of the surface.

The hypothetical sequence depicted in Fig. 1 is based on these guidelines, and the initial embryo is a fairly smoothly curving shell with a 5/6-ring ratio close to 12/20 (presumably an optimum under certain conditions based on the formation and stability of C_{60}^{B}). As the structure grows, flat segments develop, resulting in a mis-shapen, shell-like nucleus with a 7–10 Å diameter spiral (Fig. 1*d*), which is probably the minimum size for a suitable growth core. Larger initial structures may occur and their preponderance could depend on nucleation conditions.

To predict the likely shapes of the resulting particles, various large cages have been constructed. Schematic diagrams of C_{60}, C_{240} and C_{540} (of diameters 1*D*, 2*D* and 3*D*, where *D* is that of C_{60}), related to the Goldberg polyhedra[13–15], are depicted in Fig. 2. The main structural features of $C_{1,500}$ and $C_{6,000}$ are to be found in C_{540}. These cages show a major structural feature as the cages grow, the round shape disappears and flat faces develop rapidly. Even though there are only 12 pentagons in any given shell (the number of hexagons is proportional to D^2), they exert a profound influence on the shapes of the large shells. The corannulene configuration introduces a rigid cusp in the surface, the shape of which is determined by the carbon–carbon aromatic bond lengths[16]. The graphitic sheet linking the 12 pentagons follows the tangential angles which radiate out from the saucer-shaped cusps, and warps so as to maintain as planar an interlinking surface as possible. The resulting shape is quasi-icosahedral in that it consists of 20 more-or-less flat, but smoothly interconnected, triangular planes. The cross-section of a large symmetric cage is a 6–10 sided polygon, depending on the cut, and in a random-growth scheme, unsymmetric polyhedra with $\sim 8 \pm 2$-sided polygonal cross-sections should occur.

For a large particle consisting of a spiral surface based on concentric polyhedral segments, epitaxial growth causes the triangular planes in successive shells to lie directly above one-another, and the interconnecting folds to lie in triangular planes radiating from the nucleus. The model thus predicts a quasi single-crystal particle composed of 20 pyramidal microcrystallite segments. The flat layers out of which any one microcrystallite is formed fold smoothly into the layers of the three abutting microcrystallites, and are parallel to the outer surface. Due to epitaxy, the cross-section should exhibit a spiral pattern of concentric, aligned polygons, albeit with defects.

These predictions can be tested experimentalty. In 1980 Iijima[4] published TEM pictures of spheroidal carbon particles. A highly sperical example is shown in Fig. 3*a*, and a less regular and more clearly polyhedral one in Fig. 3*c*. A planar array four or five atoms wide, within a 2 Å-thick wall, parallel to the TEM beam, manifests itself as a dark line[4]. This condition can be met

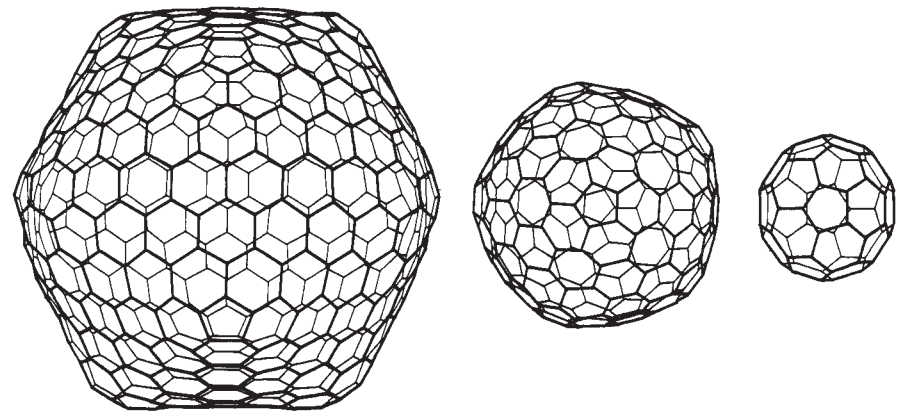

Fig. 2 A set of models for the closed symmetric fullerenes C_{60}, C_{240} and C_{540}. The diameters of the latter cages are 2 and 3 times that of C_{60}. The rapid shift towards quasi-icosahedral symmetry is striking.

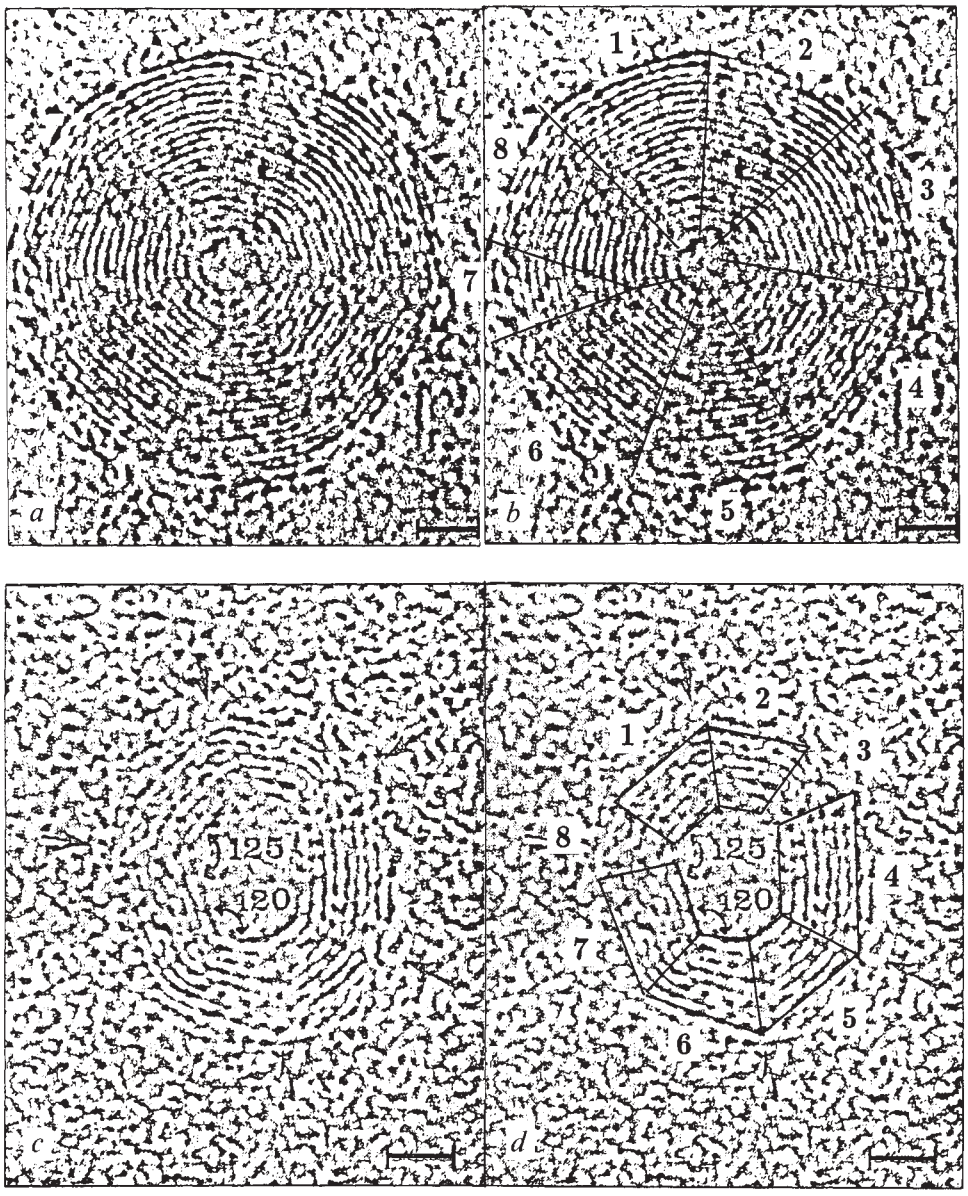

Fig. 3 *a*, *c*, Images of two published micrographs. On the right (*b*, *d*) these images are marked to delineate the features consistent with pyramidal layered microcrystallite cross-sections, as predicted. 20 Å markers are appended.

by almost any contour of a cage. Iijima has recently discussed a small central structure in one of his particles[17] which we interpret as an embryo of the kind shown in Fig. 1*d*.

The TEM patterns in Fig. 3 can now be readily explained. In the region of the nucleus in Fig. 3*a* there are discontinuities as well as curved and straight contours, consistent with an embryo such as Fig. 1*d*. Triangular segments that are consistent with cross-sections through pyramidal microcrystallites are delineated in Fig. 3*b*. Smooth-layer inter-connections are clearly visible at the 2/3 boundary and less so at the 8/1, 1/2 and 4/5 boundaries. Discontinuities, as expected, are seen in several regions, such as the 3/4, 5/6, 6/7 and 7/8 boundaries. Segment 7 appears to originate from a secondary growth point some 30 Å out from the centre, indicating the possibility of secondary and multiple growth-sites. Discontinuities near the cusps could result from incomplete formation of corannulene configurations by avoidance of pentagon formation. The angles expected should vary roughly between those for the isocahedral dihedral angle 138.2° (ref. 18), and that for corannulene of 122.8° (ref. 16). All the Iijima micrographs are consistent with polyhedral structures. Here we see that the closure criterion[9,10,11] is satisfied most simply on a microscopic scale at the cusps using only sp^2 bonding.

The particle in Fig. 3*c* is clearly polyhedral with distinct layer patterns in segments 1, 2, 4, 5, 6 and possibly 7, and discontinuities in 3, 7 and 8. The central spiral is 30–40 Å across, significantly larger than that in Fig. 3*a* and, as predicted, more distinctly polyhedral. The smaller the embryo, the more spheroidal the ultimate particle may be. Conglomerates resulting from multiple growth sites are explained by a straightforward extension of the model.

The close relationship between carbon chains and particles in circumstellar shells[19–21] led to the discovery of C_{60}^{B} (refs 6, 22) and ultimately to the present polyhedral structure proposal. Circumstellar dust is ejected into space, and so it is possible that such polyhedral particles are the primary refractory cores which are the accretion sites linking the gaseous component of the interstellar medium with large objects such as planets and stars. Also, it is likely that the symbiotic triangular relationship observed in the laboratory between polyyne chains, polyhedral shell particles and C_{60}^{B}, also exists in the interstellar medium. As C_{60}^{B} can apparently withstand destruction better than any other chemically bound species[21–25], it is likely to be distributed as ubiquitously in the Galaxy (probably ionized) as dust and chains[26,27]. Admixed hydrogen will perturb the spiral structures, although not seriously if refractory carbonaceous particles occur

at all. Hydrogenated polyhedral shells are essentially three-dimensional polyaromatic hydrocarbons (PAH) and should show PAH-type infrared emission[28]. Thus, partially hydrogenated particles are possible carriers of the Unidentified Infrared Emission Features which have features in common with those of PAH material[29].

The relationship between chains, grains and C_{60}^{B} in space seems to be paralleled in that of acetylenes with soot[19]. This possibility is supported by the discovery of C_{60}^{+} in a sooting flame[30]. Hydrogen complicates matters, probably making oxidative coupling more important in the polymerisation reaction step than free radical condensation, and perhaps obscuring some of the structural details of the resulting particles. It is unlikely that the overall mechanics of the soot-formation process differ much from that proposed here, because Iijima's particles and soot have so much in common, and two parallel processes to form such similar and unusual structures would be unlikely. The mechanism is readily modified for hydrocarbon combustion by realizing that soot should form when there is oxygen starvation, and the temperature is such that the large C—C bond energy, relative to C—H and C—O, ensures that hydrogen and oxygen insertion cannot compete with carbon-network formation. The study thus implies that soot should also show a quasi-icosahedral spiral layer structure, albeit modified by H and O inclusion, a proposal supported by the plethora of 5-membered ring compounds found in tars[31]. As for kinetic factors, it is likely that the surface accretion step is rate-limiting, as polyyne cross-linking is very fast, indeed explosive, and so the model is consistent with a growth rate proportional to the surface area of the particle.

Finally, the structures considered here rather curiously possess both icosahedral and helical features. If they are soot-like, they must have been abundant in the Earth's early atmosphere, providing useful prebiotic nucleation sites.

We acknowledge correspondence with Sumio Iijima and thank him for allowing us to use his data. We are also grateful to Paul Calvert, Kappa Cornforth, John Murrell, Lawrence Dunne, John Pethica, David Walton and Steve Wood for discussion.

Received 16 September; accepted 4 December 1987.

1. Heidenreich, R. D., Hess, W. M. & Ban, L. L. *J. appl. Crystallogr.* **1**, 1-19 (1968).
2. Marsh, P. A., Voet, A., Mullens, T. J. & Price, L. D. *Carbon* **9**, 797-805 (1971).
3. Prado, G. & Lehaye, J. *J. chim. Phys.* **72**, 483-489 (1975).
4. Iijima, S. *J. Crystal Growth* **50**, 675-683 (1980).
5. Tesner, P. A. *Symp. Faraday Soc.* '*Fogs and Smokes*' **7**, 104-108 (1973).
6. Kroto, H. W., Heath, J. R., O'Brien, S. C., Curl, R. F. & Smalley, R. E. *Nature* **318**, 162-163 (1985).
7. Kroto, H. W. *Nature* **329**, 529-531 (1987).
8. Zhang, Q. L. *et al. J. phys. Chem.* **90**, 525-528 (1986).
9. Thompson, D. W. *On Growth and Form*, Ch. 9, 737 (Cambridge University Press, 1942).
10. Jones, D. E. H. *New Scient.* **32**, 245 (1966).
11. Jones, D. E. H. *The Inventions of Daedalus* 118-119 (Freeman, Oxford, 1982).
12. Schmalz, T. G., Seitz, W. A., Klein, D. J. & Hite, G. E. *J. Am. chem. Soc.* (in the press).
13. Fowler, P. W. *Chem. phys. Lett.* **131**, 444-450 (1986).
14. Goldberg, M. *Tohoku Math. J.* **43**, 104 (1937).
15. Klein, D. J., Seitz, W. A. & Schmalz, T. G. *Nature* **323**, 703-706 (1986).
16. Barth, W. E. & Lawton, R. G. *J. Am. chem. Soc.* **93**, 1730-1745 (1971).
17. Iijima, S. *J. phys. Chem.* **91**, 3466-3467 (1987).
18. Coxeter, H. S. M. *Regular Polytopes* (Macmillan, New York, 1963).
19. Kroto, H. W. *Chem. Soc. Rev.* **11**, 435-4 (1982).
20. Kroto, H. W. *Int. Rev. phys. Chem.* **1**, 309-3 (1981).
21. Kroto, H. W., Heath, J. R., O'Brien, S. C., Curl, R. F. & Smalley, R. E. *Astrophys. J.* **314**, 352-355 (1987).
22. Kroto, H. W. *Proc. R. Instn.* **58**, 45-72 (1986).
23. Heath, J. R., O'Brien, S. C., Curl, R. F., Kroto, H. W. & Smalley, R. E. *Comments cond. Matter Phys.* **13**, 119-141 (1987).
24. Heath, J. R., O'Brien, S. C., Curl, R. F., Kroto, H. W. & Smalley, R. E. *Acc. chem. Res.* (in the press).
25. O'Brien, S. C., Heath, J. R., Curl, R. F., Kroto, H. W. & Smalley, R. E. *Chem. Phys. Lett.* **132**, 99-102 (1986).
26. Kroto, H. W. *Phil. Trans. R. Soc.* (in the press).
27. Kroto, H. W. *Polycyclic Aromatic Hydrocarbons and Astrophysics* 197-203 (eds Leger, A. *et al.*) (NATO ASI/Reidel, Dordrecht, 1987).
28. Salisbury, D. W., Allen, J. E., Donn, B., Moore, W. J. & Khanna, R. K. *Carbon in the Galaxy* (NASA Ames Conf. Proc., 1987).
29. Leger, A. & Puget, J. L. *Astr. Astrophys.* **137**, L5 (1984).
30. Gerhardt, P., Löffler, S. & Homann, K. H. *Chem. Phys. Lett.* **137**, 306-309 (1987).
31. Clar, E. *Polycyclic Hydrocarbons* (Academic, London, 1964).

Formation of highly orientated graphite from polyacrylonitrile by using a two-dimensional space between montmorillonite lamellae

Takashi Kyotani, Naohiro Sonobe & Akira Tomita

Chemical Research Institute of Non-Aqueous Solutions, Tohoku University, Katahira 2, Sendai 980, Japan

Carbon materials have many attractive physical and chemical properties, because of a wide variety of chemical bonding, crystal structure and microtexture. Carbon properties can be created by selecting a preparation procedure and a raw material. For example, many new carbon materials such as exfoliated graphite, benzene-derived fibre and diamond film have come into use recently. The possibility of creating a new carbon material by a new method still remains. Here we report a novel method of preparing a highly orientated graphite from polyacrylonitrile (PAN) by making use of the interlamellar opening of montmorillonite (MONT) as a two-dimensional space for carbonization. A MONT–PAN intercalation compound was prepared and heat-treated at 700 °C to produce carbon from PAN between MONT lamellae. The carbon was then released from MONT by acid treatment and subjected to further heat treatment at various temperatures up to 2,800 °C. The interplanar spacing (d_{002}) of the carbon treated at 2,800 °C was very close to that of ideal graphite crystal and the crystallite size, L_c and L_a, were ~40 nm and >1 μm, respectively. The formation of such a highly orientated carbon is probably a consequence of the orientation of the two-dimensional carbon precursor produced between the lamellae of MONT. When PAN itself is heat-treated, it produces a three-dimensional carbon with a network of intertwined ribbons of stacked graphitic sheets.

MONT is a typical layered clay mineral which forms intercalation compounds with various kinds of polar organic molecules. We attempted to use a two-dimensional opening between the lamellae of MONT as a carbon-producing centre intercalated polymer compounds, expecting to obtain a low-dimensional carbon which may have interesting properties[1-3].

For this purpose, we first prepared MONT(Ca form)-acrylonitrile complex[4,5], using 0.14 g of intercalated monomer per gram of MONT. The complex was subjected to γ-ray radiation at room temperature under nitrogen to polymerize acrylonitrile between the lamellae. The formation of PAN was confirmed by Fourier transform infrared measurements. The MONT-PAN complex was then heat-treated under flowing nitrogen. *In situ* X-ray diffraction measurements revealed that the interlamellar spacing of the complex was ~1.3 nm below 300 °C, a spacing which corresponds to the presence of monolayer PAN. The polymer decomposed between 400–550 °C and formed flat carbonaceous molecules, and this change resulted in a slight

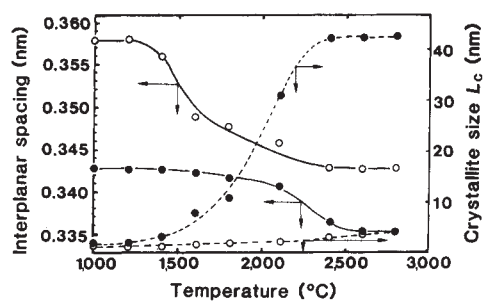

Fig. 1 Changes of the interplanar spacing d_{002} and the crystallite size, L_c, of IPC (●) and FPC (○) as a function of HTT.